July 14, 1997 version

Neutron Studies of Nanostructured CuO-Al_2O_3 NOx Removal Catalysts*

Masakuni Ozawa[1] and Chun-Keung Loong[2]

[1]Nagoya Institute of Technology, Tajimi, Gifu 507, Japan,

[2]Argonne National Laboratory, Argonne, Illinois 60439, U.S.A.

Abstract

Nanostructured powders of automotive catalytic system CuO-Al_2O_3, targeted for nitrogen oxides (NOx) removal under lean-burn engine conditions, were investigated using neutron diffraction and small-angle neutron scattering. The crystal phases, structural transformations and microstructure of 10 mol% Cu-Al_2O_3 powders are characterized according to the heat-treatment conditions. These properties are correlated with the pore structure and NOx removal efficiency determined by nitrogen adsorption isotherm, electron spin resonance, and temperature programmed reaction measurements. The γ-$(Cu, Al)_2O_3$ phase and the mass-fractal-like aggregate of particles (size $\approx$ 26 nm) at annealing temperatures below 900°C were found to be crucial to the high NOx removal performance. The transformation to bulk crystalline phases of α-Al_2O_3 + $CuAl_2O_4$ spinel above ~1050°C corresponds to a drastic drop of NOx removal efficiency. The usefulness of neutron-scattering techniques as well as their complementarity with other traditional methods of catalytic research are discussed.

Keywords: alumina catalyst; copper modified alumina, nitrogen oxides; automotive exhaust

---

*An invited paper

Corresponding author: Masakuni Ozawa, Nagoya Institute of Technology, CRL, Asahigaoka, Tajimi, Gifu 507, Phone: 81-572-27-6811, FAX: 81-572-27-6812, e-mail: ozawa@crl.nitech.ac.jp

DISCLAIMER

1. Introduction

The requirement for reaction-specific, high-performance catalysts often demands the use of complex materials, such as metal-exchanged zeolites or nanophase metal-oxide solid solutions. While information concerning the reaction mechanisms and electronic states of reactive species is traditionally obtained from temperature programmed reaction studies and similar methods, the understanding of the crystal phases and microstructure relies on a variety of experimental techniques. Electron microscopy yields real-space images of organization of crystalline particles or phase components over a small volume of the samples. Neutron scattering, on the other hand, reveals structural information of macroscopic samples formulated in the neutron wavevector (Q) space. Through a Fourier transform, the crystal phase morphology, aggregation of primary and secondary particles, and agglomeration of aggregates can be characterized over the length scale of 0.1-500 nm. In recent years, we have witnessed the increasing applications of neutron-scattering techniques for industrial research.[1] The realization of these applications, to a large extent, is due to the development of a variety of neutron instruments which are made available to users at many facilities. In this paper, we hope to demonstrate the usefulness of neutron characterization of nanostructured copper-modified aluminas for the development of nitrogen oxides (NOx) removal catalysts for lean-burn engines.

Cu-Al_2O_3 and Cu ion exchanged ZSM-5 zeolite have been reported to be effective for the selective reduction of NOx in the presence of some reductants despite an excess of oxygen and large space velocity.[2-5] They are alternative NO removal materials suitable to the so-called lean-burn engines. The industrial goal is to develop practical three-way catalytic converters for lean-burn automobile engines, leading to massive reduction of green-house

gases and a relief of global warming. It appears that zeolite-based catalysts have low stability under hydrothermal conditions over about 800°C, therefore, the durability of a three-way automotive catalyst is seriously reduced under normal engine operation at temperatures between 100 to 1000°C. The stabilization of active copper species at elevated temperatures is currently one of the important research areas in Cu-exchanged zeolite-based lean-burn de-NOx catalysis. γ-Al_2O_3 has been widely applied to coat-layers supporting promoters in automotive three-way converters. In a recent study of the solid-state thermal behavior and the NO removal performance of Cu-modified Al_2O_3 under lean-burn conditions, we found evidence of Cu-induced bulk-state structural modification of alumina related to the improvement of thermal durability.[6-8] Here we report the crystal phases and microstructure of these catalysts by neutron diffraction and small-angle scattering. The neutron data are correlated with results from parallel measurements of nitrogen isotherm adsorption and NOx removal activities.

2. Experimental

The γ-Al_2O_3 powders have a surface area of 115 m^2/g and a purity of 99.9%. The 10 mol% Cu-Al_2O_3 (i. e., $Cu/Al_2O_3 = 0.1$) samples were prepared by impregnation of the γ-Al_2O_3 powder with aqueous copper nitrate solution, followed by agitation of the suspension, and drying at 110°C. The products were heated in air at 500°C for 3 h, re-ground and further heated at selected temperatures up to 1100°C in air for 3 h.

Neutron diffraction (ND) experiments were carried out using the General Purpose Powder Diffractometer (GPPD) at the Intense Pulsed Neutron Source (IPNS) of Argonne National Laboratory. A heat-treated, pure Al_2O_3 or 10 mol% Cu-Al_2O_3 powder sample was enclosed in a thin-wall vanadium can (11 mm diameter, 50 mm long) for room-temperature

measurements. A resolution of $\Delta d/d = 0.25\%$ (where d is the atomic spacing) can be achieved from a backscattering geometry at a mean scattering angle (2θ) of $\pm 148°$. For the present samples with small grains, resolution effect is not a limiting factor to data analysis.

The small-angle neutron scattering (SANS) experiments were carried out using the SAND diffractometer also at IPNS.[9] Incident neutrons with wavelengths in the range of 0.05-1.4 nm were used and the sample-to-detector distance of 1.54 m was fixed throughout the experiment. The scattered neutron intensities as a function of position and time were recorded by using a gas-filled area detector and time-of-flight techniques. The sample was enclosed in a Suprasil cell (sample thickness 1 mm) and controlled at a temperature between ambient temperature and 500°C. The data were corrected for background and empty-cell scattering as well as detector nonlinearity and were normalized by using the known scattering cross section of a silica gel standard. A good Q-resolution (root-mean-square deviation varying from about 0.001 to 0.012 $Å^{-1}$ over the observed Q-range of 0.007 - 0.03 $Å^{-1}$) was achieved without altering the sample-to-detector configuration. We find no noticeable effect of instrumental resolution on the interpretation of the present data.

The adsorption-desorption isotherm of nitrogen on the powders at 77K (Autosorb, Quantachrome, USA) was measured as a function of relative pressure. Before the measurement, the sample was outgassed at ~150°C under vacuum for 8h. The pore distribution was obtained from the desorption isotherms assuming cylindrical pore shape.

Catalytic removal activity of catalysts was examined using gas mixtures containing nitrogen monoxide and hydrocarbons (HC) with a large space velocity (gas-flow rate per unit volume of catalyst) of 100,000/h, simulating an automotive exhaust under a fuel-lean condition at an air/fuel ratio of 18, as previously described.[6] The dispersion of Cu(ll) cations in a

sample was monitored by an electron spin resonance (ESR) spectrometer (JEOL-3MX, Japan) at room temperature in an X-band with a modulation frequency of 100 kHz.

3. Results and Discussion

3.1 Catalytic NO removal activity

Table 1 summarizes the NO and C_3H_6 removal conversion efficiencies (maximum values), as well as the surface areas and pore structure derived from the BET method, for the Cu-Al_2O_3 powders heat-treated at 500°, 900° and 1100°C for 3h in air. The NO and HC conversion rates as a function of gas-inlet temperature are usually correlated so that the NO removal efficiency reaches a maximum only within certain temperatures (300 - 350°C for the present system). The data suggest that an NO removal activity of 20% maintains for the sample heated at 900°C, but decreases drastically to less than 3% after a heat treatment above 1050°C. Since Cu-ion exchange zeolite catalysts decompose and lose NOx removal activity above ~650°C, the heat-durability for the Cu-modified alumina catalyst provides a distinct advantage. It is of crucial importance to understand the evolution of crystal phases and microstructure over the 500° - 1100°C heat-treatment temperatures and the possible relationship with the NOx removal performance.

3.2. Neutron diffraction

Transitions of various crystalline phases of alumina occur over a wide range of temperatures (~300-1200°C). Depending on the chemical routes in synthesis, heat-treatment temperatures, atmospheric conditions and other factors, these intermediate phases, collectively referred to as transition aluminas, often coexist in a gel or powder. Furthermore, doping a small amount of transition-metal oxides in alumina often alters the formation of transition aluminas.

For example, addition of 1 mol% of La in Al_2O_3 effectively shifts the α-phase formation temperature from ~1125°C for pure alumina to ~1250°C, probably due to the larger size of La than Al ions which hinders ionic diffusion in the processes of sintering and transformation.[10] The ability of tailoring of the catalytic functions of active alumina by means of modifying its surface and/or bulk states through impregnation or alloying is one of the most important goals targeted by researchers.

We investigated the crystal phases of the 10 mol% Cu-Al_2O_3 samples heat-treated at 500°, 920°, 930°, 950°, 1000°, 1050°, and 1100°C. Fig. 1 displays a portion of the observed, background-subtracted and fitted powder patterns of 10 mol% Cu-Al_2O_3 heat-treated at 500°, 920°, and 1100°C. First, the narrowing of the peaks with increasing annealing temperature is indicative of coarsening of crystalline domains. Second, complex structural phase transformations occur over the 500° - 1100°C temperature range. Below about 1050°C the transitions are sluggish as the large fluctuations of surface energies across particles diversify atomic migrations. The diffraction patterns between the coexisting phases are similar because the structures are mainly governed by the relative occupations of Al atoms among the tetrahedral and octahedral sites defined by the packing of O atoms. The fits in Fig. 1 are based on a mixture of CuO and γ-Al_2O_3 for annealing at 500°C, a θ- Al_2O_3 plus an oxide solid solution of Cu and Al with the γ-phase symmetry at 920°C, and a mixture of α-Al_2O_3 phase and $CuAl_2O_4$ spinel at 1100°C. The formation of the $CuAl_2O_4$ phase occurs between 1000° and 1100°C. Previous studies have shown evidence of the formation of a "surface spinel" that has different cation distribution from the bulk $CuAl_2O_4$ structure.[11, 12] Based on the well defined peak shape and the satisfactory refinement, we conclude that the $CuAl_2O_4$ structure at 1100°C is a bulk spinel

phase. Currently, we are undertaking a systematic comparison of the neutron and x-ray results in the attempt to understand the interplay of the surface and bulk phases as a function of the Cu content and annealing temperature.

3.3 Small angle scattering

SANS permits the determination of mean particle size and the nature of the aggregate in terms of the particle form factor and interparticle correlation. Information about polydispersity can be obtained from fitting the data with a model and a size-distribution function. The data analysis is based on a mass-fractal model which was successfully applied to the case of rare-earth modified zirconia powders previously.[13-15] Since the rationale of such an analysis has been given in detail elsewhere, we only outline the results here. Fig. 2 shows the SANS data in terms of log-intensity versus log-Q profiles for pure γ-Al_2O_3 and heat-treated Cu-Al_2O_3 of selective annealing temperatures. The lines represent the fits of the data to the mass-fractal model which contains six parameters: the mean particle radius (R), fractal cutoff distance (ξ), fractal dimension (D), geometric standard deviation of the log-normal size distribution (σ), a prefactor, and a Q-independent background. Table 2 lists the parameters for different samples obtained from the fits. All the data sets with the exception of the Cu-Al_2O_3 heat-treated at 1100°C can be described adequately by the model. We find that the mean particle size (2R) varies from about 11 to 36 nm as the annealing temperature increases from 500° to 1050°C. The fractal cutoff distance decreases from 29 nm at 500°C to values comparable to the particle size at temperatures above 900°C. Since, by definition, the ξ represents the distance beyond which the density of the fractal object approaches the macroscopic density, $\zeta \approx 2R$ does not make physical sense. However, the mean particle size and size distribution, which are characterized by the

position and shape of the broad maximum in the log-log plots, remain accurate. The particle-size distribution of all the powders are broad, corresponding to a $\sigma \approx 1.5$ for the log-normal distribution. The fractal dimension appears to increase with increasing annealing temperature (see Table 2). All of these observations are consistent with the interpretation that particles coarsen and density by heating.

The intensity profile of the Cu-Al_2O_3 heat treated at 1100°C shows a distinctly different shape (see Fig. 2), and an attempt in fitting the data with the fractal model failed completely. An rough estimate of the particle size using a model of hard spheres resulted in a minimum particle size of 100 nm. Not surprisingly, such drastic change of the microstructure between 1050° and 1100°C coincides with the formation of well-grown α-Al_2O_3 and $CuAl_2O_4$ phases, as confirmed by diffraction (Fig. 1). The slope of the log-log plot over the Porod regime (QR>>1) provides a measure of the surface roughness of the constituent particles in an aggregate. A slope of -4 indicates smooth surface and a value between -3 and -4 implies rough fractal-like surface. Such values obtained from power-law fit at large Q are given in Table 2. It can be seen that the slopes for the two powders heat-treated at 500°C are close to 3.8 whereas those for the higher annealing temperatures are close to 4.0. This suggests a certain degree of surface roughness of particles within the micro- and mesoporous microstructure for the powders heated at low temperatures (< 500°C). At annealing temperatures above ~900°C, the powders consist of larger and smoother particles resulted from sintering.

3.4 Pore structure

Fig. 3 shows the pore distribution in terms of the pore-volume-log-radius versus pore radius of Cu-Al_2O_3 heated at 500°, 900° and 1100°C obtained from BET analyses of the desorption isotherm data. The mean pore radius and pore volume are listed in Table 1. The

shape of the pore distributions is consistent with a log-normal distribution. After heat treatment at 1100°C, the powder is devoid of microporosity or mesoporosity (pore radius below 20 nm). Only macropores of micrometer size remain. Clearly, this development is resulted from the $\gamma \rightarrow \alpha$-$Al_2O_3$ transition and the formation of $CuAl_2O_4$ at ~1050°C, yielding a random packing of large solid particles.

3.5 Nanostructure and catalytic properties

The ESR spectrum of the Cu-Al_2O_3 heated at 500°C implies the presence of Cu(II) ions coordinated with open octahedron oxygens on the surface of the particles. At higher temperatures, additional features corresponding to g-factors of 2.1 and 2.3 appeared but the overall results are consistent with only Cu(II) ions in various solid states coordinated by mainly oxygen atoms. It is noteworthy that the NO removal coefficients are similar for the 500°C and 900°C heat-treated Cu-Al_2O_3 despite of a large decrease in surface area in the latter sample. In light of the neutron results, the crystal morphology and the almost fractal-like aggregate with micro- and mesoporous structure common to all the samples annealed at temperatures below 1100°C appear to play an important role in the NOx removal activity.

4. Summary

Automotive catalytic powders of the CuO-Al_2O_3 system, designated for NO removal under lean-burn engine conditions, were investigated by neutron diffraction and small-angle scattering for the purpose of determining the microstructural evolution, phase transitions and thermal durability of the catalysts. A sequence of γ-Al_2O_3 + CuO to γ-phase $(Cu, Al)_2O_3$ solid solution to α-Al_2O_3 + $CuAl_2O_4$ transformations were identified with the corresponding heat-treatment temperatures. The evolution from the almost mass-fractal-like aggregate of crystalline

particles with micro- and mesoporosity to a random packing of coarsened, solid particles was observed. These observations, as considered in conjunction with results from nitrogen adsorption isotherm, ESR and NO removal measurements, indicate that the low-temperature phases and the fractal-like aggregate are important to the high efficiency of NO conversion. We demonstrated the usefulness of neutron scattering method for industrial research of novel catalytic materials.

Acknowledgment

We thank J. Ku, P. Thiyaga, R. Thomas, J. W. Richardson, Jr., and D. Wozniak for their help in the neutron experiments. MO thanks Professor S. Suzuki for his encouragement. Work performed at Argonne National Laboratory is supported by the U. S. DOE-BES under Contract No. W-31-109-ENG-38.

References

1. S. K. Sinha, D. J. Lohse, and M. Y. Lin, Physica **B 213&214**, 1 (1995).
2. M. Iwamoto and H. Hamada, Catal. Today **10**, 57 (1991).
3. H. Hamada, Y. Kintaichi, M. Sasaki, and T. Ito, Appl. Catalysis B **70**, L15 (1991).
4. H. Hamada, Y. Kintaichi, M. Sasaki, and T. Ito, Appl. Catalysis B **75**, L1 (1991).
5. W. Held, A. Konig, T. Richter, and L. Puppe, in *SAE paper No. 900496* (Soc. Automotive Eng., 1990).
6. M. Ozawa, H. Toda, O. Kato, and S. Suzuki, Appl. Catalysis B **8**, 123 (1996).
7. M. Ozawa, S. Suzuki, C.-K. Loong, J. W. Richradson, Jr., and R. R. Thomas, App. Surf. Sci. **in press** (1997).
8. M. Ozawa, H. Toda, and S. Suzuki, Appl. Catalysis B **8**, 141 (1996).
9. P. Thiyagarajan, J. E. Epperson, R. K. Crawford, J. M. Carpenter, T. E. Klippert, and D. G. Wozniak, J. Appl. Cryst. **30**, 208 (1997).
10. C.-K. Loong, J. W. Richardson, Jr., and M. Ozawa, J. Alloys Compounds **250**, 356 (1997).
11. R. M. Friedman, J. J. Freeman, and F. W. Lytle, J. Catal. **55**, 10-28 (1978).
12. B. R. Strohmeier, D. E. Leyden, R. S. Field, and D. M. Hercules, J. Catal. **94**, 514 (1985).
13. C.-K. Loong, P. Thiyagarajan, J. Richardson, J. W., M. Ozawa, and S. Suzuki, J. Catal. , to be published.
14. S. K. Sinha, Physica **D 38**, 310 (1989).
15. J. Teixeira, J. Appl. Cryst. **21**, 781 (1988).

Table 1. Catalytic properties, surface areas and pore volumes of 10 mol% Cu-Al_2O_3 powders. Removal coefficients for nitrogen monoxide and hydrocarbons were measured using simulated automotive exhaust with high space velocity.

T (°C)	Maximum removal (Temperature range)		Surface area	Pore radius	Pore volume
	NO	Hydrocarbons	(m^2/g)	(nm)	(ml/g)
500	25% (300°-350°C)	100% (>400°C)	115	8.0	1.51
900	20% (300°-350°C)	100% (>400°C)	48	12.1	0.70
1100	<3% (300°-400°C)	~70% (>500°C)	3	--	0:01

Table 2. Parameters characteristic of the aggregates of pure and 10 mol % Cu-Al_2O_3 samples obtained from fitting the SANS data with a mass-fractal model.

Samples[a], annealing Temp. (°C)	Particle diameter (nm)	Fractal cutoff distance (nm)	Fractal dimension	Porod slope
γ-Al_2O_3, 500	11.14(6)	29.2(6)	2.17(1)	-3.77(10)
θ-Al_2O_3, 900	16.12(8)	26.7(8)	2.07(1)	-4.08(10)
500	11.70(6)	20.2(3)	2.32(1)	-3.91(10)
930	26.4(2)	--	--	-4.1(1)
950	26.2(2)	--	--	-4.1(1)
970	29.8(2)	--	--	-4.1(1)
1000	29.8(2)	--	--	-4.0(1)
1050	35.8(2)	--	--	-4.0(1)
1100	>100	--	--	-4.0(2)

[a]10 mol% Cu-Al_2O_3 unless specified.

Figure captions

Figure 1. Rietveld profile fits in the 0.05 to 0.3 nm region of d-spacing for the 10 mol% Cu-Al_2O_3 samples. The symbols are the observed, background-subtracted intensities. The solid line represents the calculated crystalline intensities. Tick marks of top and bottom rows indicate the positions of the Bragg reflections, respectively of (a) CuO and γ-Al_2O_3, (b) θ-Al_2O_3 and γ-$(Cu,Al)_2O_3$, and (c) $CuAl_2O_4$ and α-Al_2O_3. In (c) the three arrows indicate aluminum powder lines from the lid of the sample can.

Figure 2. The log-log plot of SANS data for the pure γ-Al_2O_3 (a) and 10 mol% Cu-Al_2O_3 samples (b-d). The heat-treatment temperatures are 500°C (a-b), 930°C (c) and 1100°C (d). The solid lines in (a-c) are fits of the data using the mass-fractal model.

Figure 3. The pore-volume-log-radius distribution function of the heated-treated 10 mol% Cu-Al_2O_3 samples.

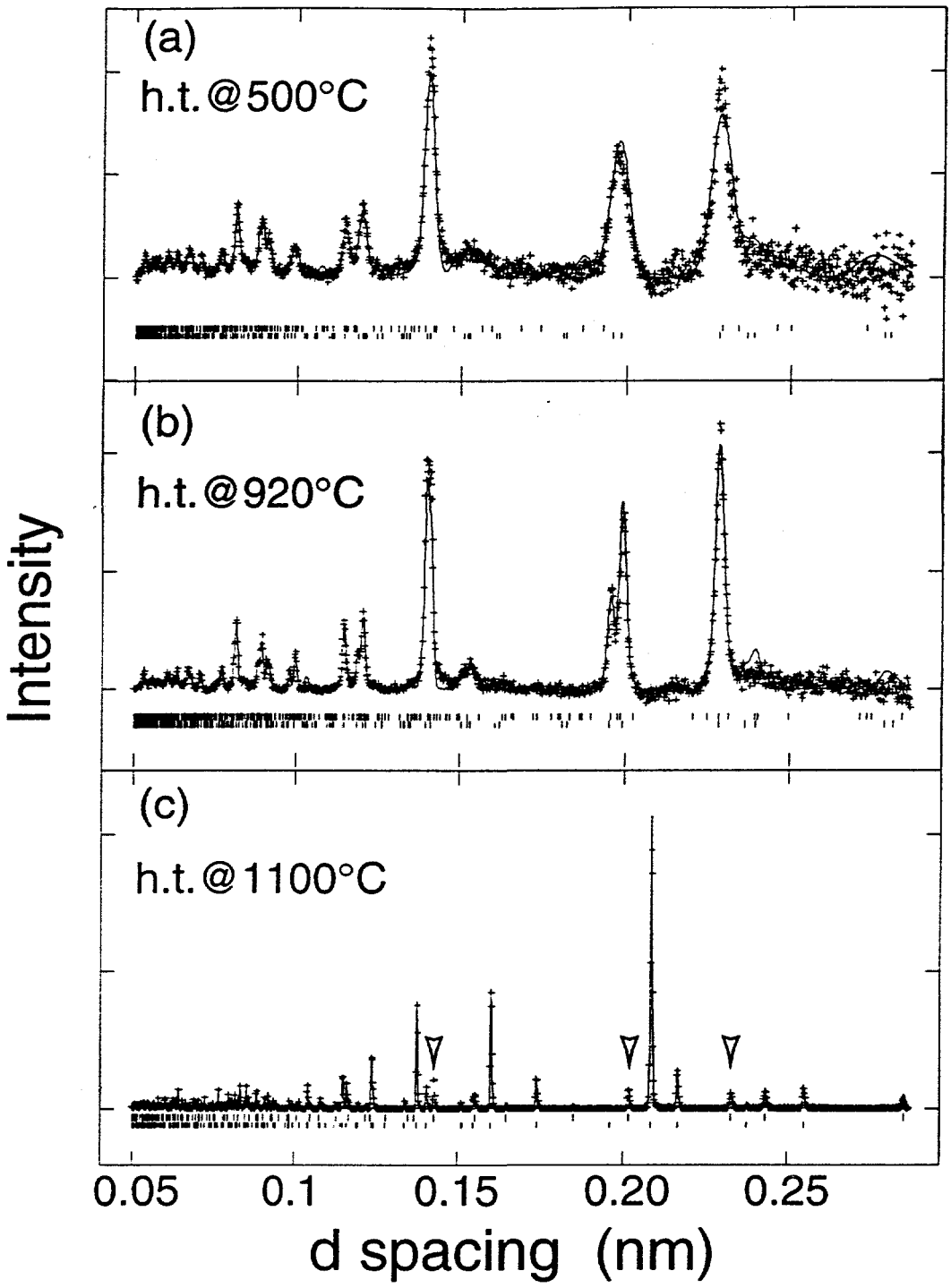

Fig. 1, Ozawa & Loong, "Neutron Studies of Nanostructured..."

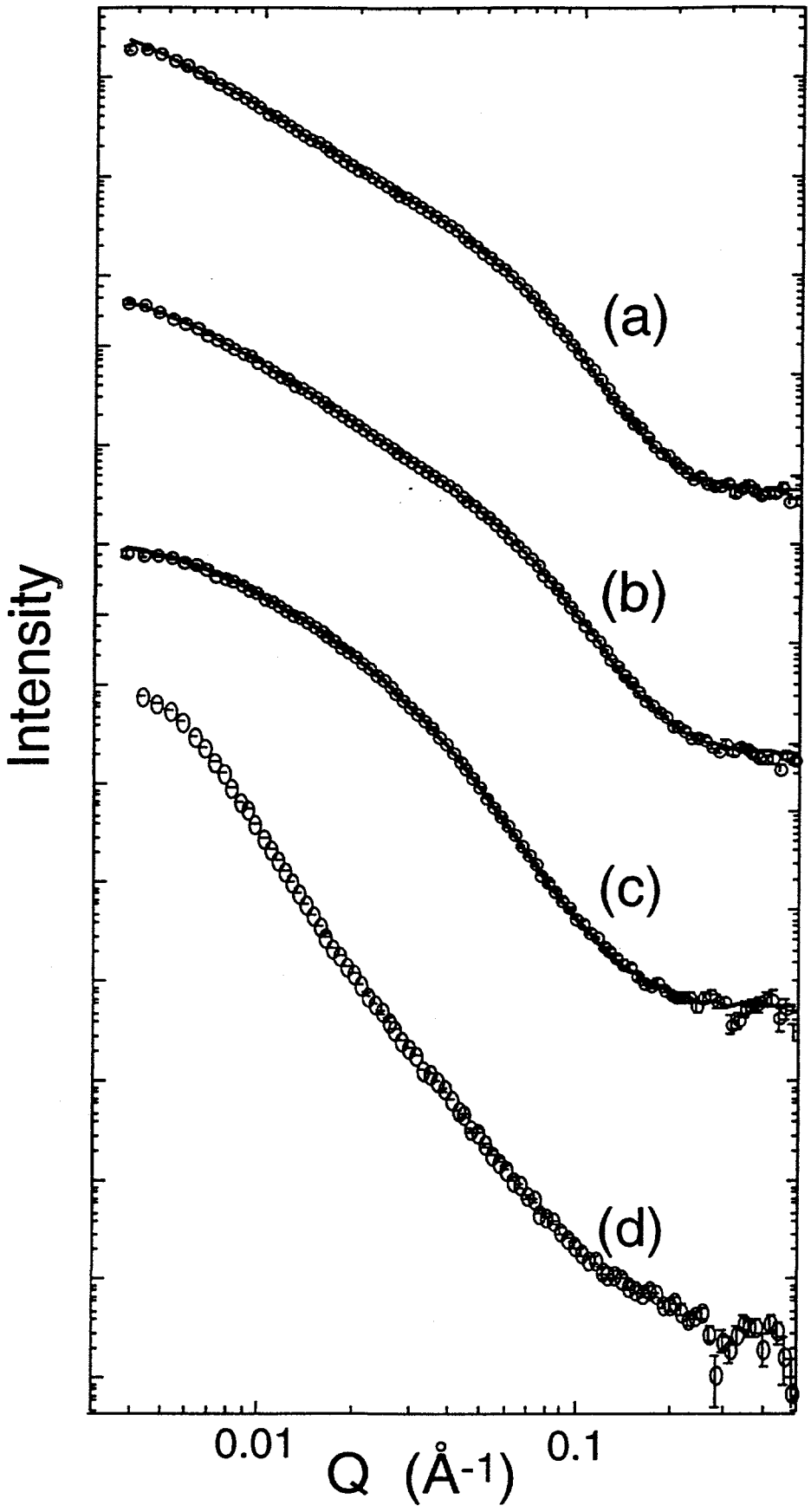

Fig. 2, Ozawa & Loong, "Neutron Studies of Nanostructured..."

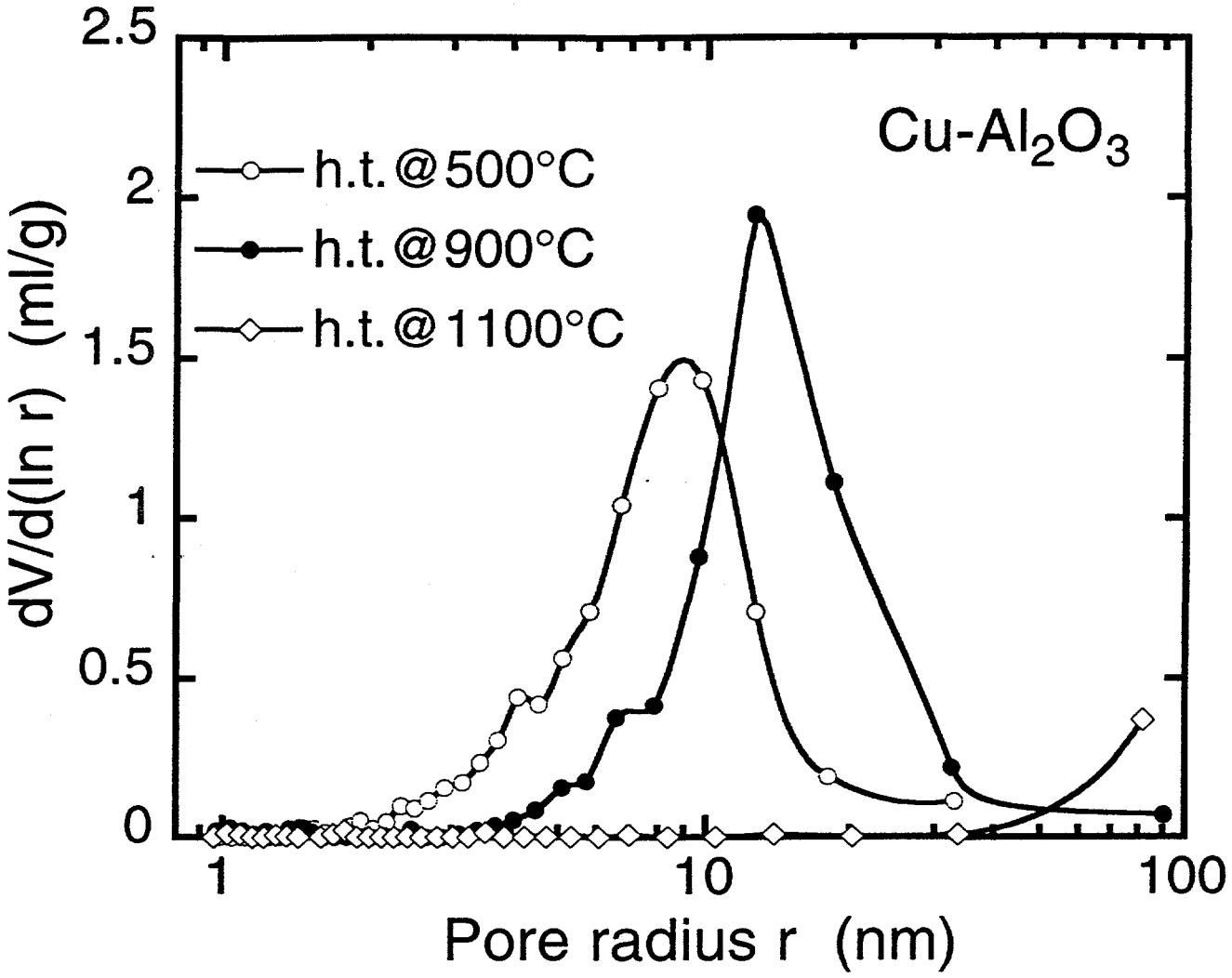

Fig. 3, Ozawa & Loong, "Neutron Studies of Nanostructured..."

Estimation of the length of this paper

a) Title, authors, affiliation and 141-word abstract	350 words
b) 3 figures, fitting a single column	450 words
c) 2 tables, single column, 22 lines	220 words
c) Manuscript text	2417 words
d) References (15)	225 words
Total:	3662 words

For six printed pages: 4800 words